RESEARCH ARTICLE

Hedgehog participates in the establishment of left-right asymmetry during amphioxus development by controlling *Cerberus* expression

Guangwei Hu[‡], Guang Li[‡], Hui Wang[*] and Yiquan Wang[§]

ABSTRACT

Correct patterning of left-right (LR) asymmetry is essential during the embryonic development of bilaterians. Hedgehog (Hh) signaling is known to play a role in LR asymmetry development of mouse, chicken and sea urchin embryos by regulating *Nodal* expression. In this study, we report a novel regulatory mechanism for *Hh* in LR asymmetry development of amphioxus embryos. Our results revealed that $Hh^{-/-}$ embryos abolish *Cerberus* (*Cer*) transcription, with bilaterally symmetric expression of *Nodal*, *Lefty* and *Pitx*. In consequence, $Hh^{-/-}$ mutants duplicated left-side structures and lost right-side characters, displaying an abnormal bilaterally symmetric body plan. These LR defects in morphology and gene expression could be rescued by *Hh* mRNA injection. Our results indicate that *Hh* participates in amphioxus LR patterning by controlling *Cer* gene expression. Curiously, however, upregulation of Hh signaling failed to alter the *Cer* expression pattern or LR morphology in amphioxus embryos, indicating that Hh might not provide an asymmetric cue for *Cer* expression. In addition, *Hh* is required for mouth opening in amphioxus, hinting at a homologous relationship between amphioxus and vertebrate mouth development.

KEY WORDS: Hedgehog, Cerberus, Left-right asymmetry, Embryonic development, Amphioxus

INTRODUCTION

Left-right (LR) asymmetry is an essential feature of embryonic development in most bilateral animals. Correct positioning of asymmetric organs along the LR axis is important for their proper function and abnormality results in heterotaxy and situs inversus (Sutherland and Ware, 2009). LR asymmetry patterning in vertebrates requires asymmetric expression of *Cerberus* (*Cer*), *Nodal*, *Lefty* and *Pitx2* in either the left or right side of embryos (Yoshiba and Hamada, 2014). During the development of embryos, *Cer* [including *Cerl2* (*Dand5*) in mice, *Coco* in frog and *Charon* in medaka] first becomes asymmetrically expressed in a L<R manner around the node (Hojo et al., 2007; Marques et al., 2004; Schweickert et al., 2010). Antagonized by Cer protein, Nodal activity then becomes biased to the left side of the node, from which a Nodal cue is transmitted unilaterally to the left lateral plate

mesoderm (LPM), where it in turn induces asymmetric expression of *Nodal*, *Lefty* and *Pitx2* (Nakamura and Hamada, 2012). The mechanism responsible for asymmetric expression of *Nodal*, *Lefty* and *Pitx2* has been analyzed in mice (Brennan et al., 2002; Marques et al., 2004; Saijoh et al., 2003). However, the molecular mechanism regulating *Cer* expression remains elusive (Yoshiba and Hamada, 2014). Interestingly, work in our lab revealed that *Cer* is also first asymmetrically expressed in developing amphioxus embryos and acts upstream of *Nodal*, *Lefty* and *Pitx* (Li et al., 2017). This finding led us to further investigate the regulatory mechanism of *Cer* in amphioxus.

In addition to aforementioned molecules, Hedgehog (Hh) signaling is also implicated in LR asymmetric development. In chick, *Shh* is asymmetrically expressed in the left side of Hensen's node, and blocking Hh activity at the node disrupts *cNR-1* (chick *Nodal* gene) expression in the LPM and LR patterning of heart laterality (Dathe et al., 2002; Levin et al., 1995; Pagán-Westphal and Tabin, 1998). The loss of Hh signaling by *Smo* gene knockout in mouse led to multiple LR defects in visceral organ patterning and in *Nodal*, *Lefty2* and *Pitx2* expression (Zhang et al., 2001). Similarly, *Hh* knockdown in sea urchin disrupted right-side *Nodal* expression and right-side characteristics, but did not affect development of left-side structures (Hojo et al., 2007; Warner et al., 2016). However, the function of Hh signaling in LR patterning remains to be elucidated in zebrafish and *Xenopus*, although left-side ectopic expression of *Shh* perturbs their LR asymmetry development (Chen et al., 1997; Sampath et al., 1997; Schilling et al., 1999). Thus, to fully understand the function of Hh signaling in LR patterning and to evaluate the conservation of this function during evolution, studies of species from other taxonomic groups are evidently needed.

Amphioxus belongs to subphylum Cephalochordata and represents the most ancient of living chordates. Owing to its vertebrate-like body plan, compact genome and similar embryonic development to that of vertebrates, amphioxus has been regarded as an valuable animal model for understanding the mechanisms of vertebrate development (Bertrand and Escriva, 2011; Koop and Holland, 2008). Amphioxus exhibits consistent LR asymmetry in pharyngeal structures at larval stages, with the mouth and preoral pit formed on the left and club-shaped gland and endostyle positioned largely on the right (Soukup et al., 2015). In addition, amphioxus embryos develop somites asymmetrically along the LR axis, with the left somites positioned more anteriorly than those on the right from the five-somite stage (Minguillon and Garcia-Fernandez, 2002). Consistent with its compact genome, amphioxus encodes only a single *Hh* homolog, representing the archetype of vertebrate *Shh*, *Ihh* and *Dhh* (Shimeld, 1999). Interestingly, *Hh* is asymmetrically expressed on the left side in amphioxus, like *Shh* in chick (Levin et al., 1995; Shimeld, 1999). Our recent study found that *Hh* knockout in amphioxus disrupts the normal placement of

State Key Laboratory of Cellular Stress Biology, School of Life Sciences, Xiamen University, Xiangan District, Xiamen, Fujian 361102, China.
*Present address: Lo Kwee-Seong Integrated Biomedical Sciences Building, The Chinese University of Hong Kong, New Territories, Hong Kong.
[‡]These authors contributed equally to this work

[§]Author for correspondence (wangyq@xmu.edu.cn)

Y.W., 0000-0002-3305-7535

several organs, such as the preoral pit and gill slits, along the LR axis (Wang et al., 2015). This implicated a role of *Hh* in amphioxus LR asymmetry establishment.

In this study, we show that *Hh* mutation in amphioxus results in morphologically symmetrical embryos, in which the left-side organs are duplicated and present on both sides, whereas the right-side structures are lost. Moreover, we examine the expression patterns of *Cer*, *Nodal*, *Lefty* and *Pitx*, and find that *Cer* expression disappears completely whereas expression of *Nodal*, *Pitx* and *Lefty* becomes bilaterally symmetric in *Hh* mutants. These results reveal a novel mechanism for *Hh* in LR patterning by regulating *Cer* expression.

RESULTS

Hh mutation disrupts the morphological asymmetry of amphioxus larvae

As described in our previous study, we obtained amphioxus $Hh^{-/-}$ mutants by inbreeding of $Hh^{+/-}$ individuals (Wang et al., 2015). When the offspring developed to mouth-open stage, ~25% exhibited a bilaterally symmetric phenotype. To establish whether this phenotype was caused by loss of *Hh* function, we performed a genotyping analysis using a PCR product cleavage assay. The results showed that the larvae with normal morphological features were $Hh^{+/-}$ or wild type (WT, i.e. $Hh^{+/+}$) (10/10), whereas those with bilaterally symmetrical features were always $Hh^{-/-}$ (10/10) (Fig. 1B). DNA sequencing of amplicons from the $Hh^{-/-}$ individuals revealed an 8 bp deletion at the TALEN target site (Fig. 1C).

Next, we carefully examined the morphological features of the offspring and found no differences between WT and heterozygous individuals until adult. The WT/heterozygous larvae develop the mouth, preoral pit, left part of the endostyle and club-shaped gland (CSG) duct on the left side of the body, with the right part of the

Fig. 1. TALEN target site of the amphioxus *Hh* gene and genotyping analysis of embryos with normal and abnormal phenotypes. (A) The amphioxus *Hh* gene. Binding sites for the TALEN pairs [forward (Fw) and reverse (Rv)] used in this study are highlight in gray. The *Bsr*GI site in the spacer is underlined. E1 to E4 indicate the four exons of the gene. (B) Gel electrophoresis of PCR products containing the target site from embryos with normal and abnormal phenotypes digested by *Bsr*GI. White arrow, uncleaved (mutant) bands; green arrow, cleaved (WT) bands. (1-10) Individuals of normal phenotype. (11-20) Individuals with bilaterally symmetric phenotype. P, undigested PCR product control. M, DNA size marker. (C) Sequencing results of *Bsr*GI cleaved (WT) and uncleaved (Mut) PCR products.
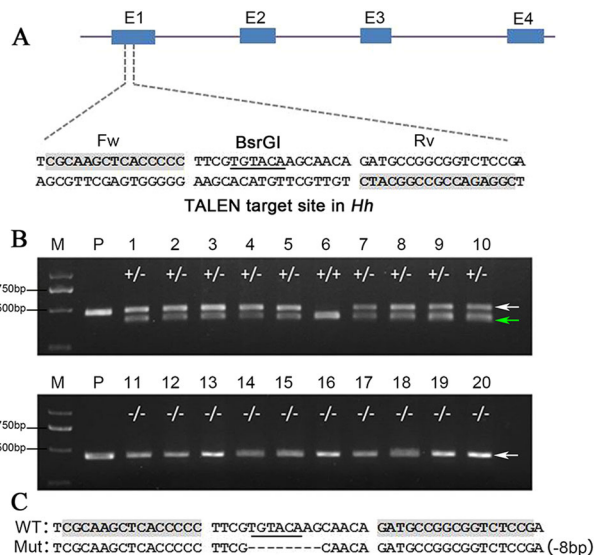
endostyle, glandular region of CSG and the first gill slit on the right side of the body (Fig. 2A-D). Their muscle segments are arranged asymmetrically in an interwoven pattern along the anteroposterior axis (Fig. 2E). However, H&E section staining showed that all $Hh^{-/-}$ larvae had gill slits ventrally but no mouth opening on either side (Fig. 2C′,D′), and SEM results indicated that the $Hh^{-/-}$ larvae developed preoral pits on both sides without mouth opening (Fig. 2F′,G′). The left part of the endostyle and the duct of CSG were also duplicated, like the preoral pit, but the right part of the endostyle and glandular region of the CSG had disappeared (Fig. 2A′-D′). In addition, the muscle segments of these homozygous mutants became symmetrically aligned on both sides of the notochord (Fig. 2E′).

We also examined the expression pattern of *Ptch*, a direct target of Hedgehog signal (Hooper and Scott, 2005), in the $Hh^{-/-}$ embryos to confirm whether the phenotype was caused specifically by the *Hh* mutation as opposed to off-target effects on other genes. As expected, *Ptch* expression was dramatically decreased in $Hh^{-/-}$ as compared with WT/$Hh^{+/-}$ embryos (Fig. 2H).
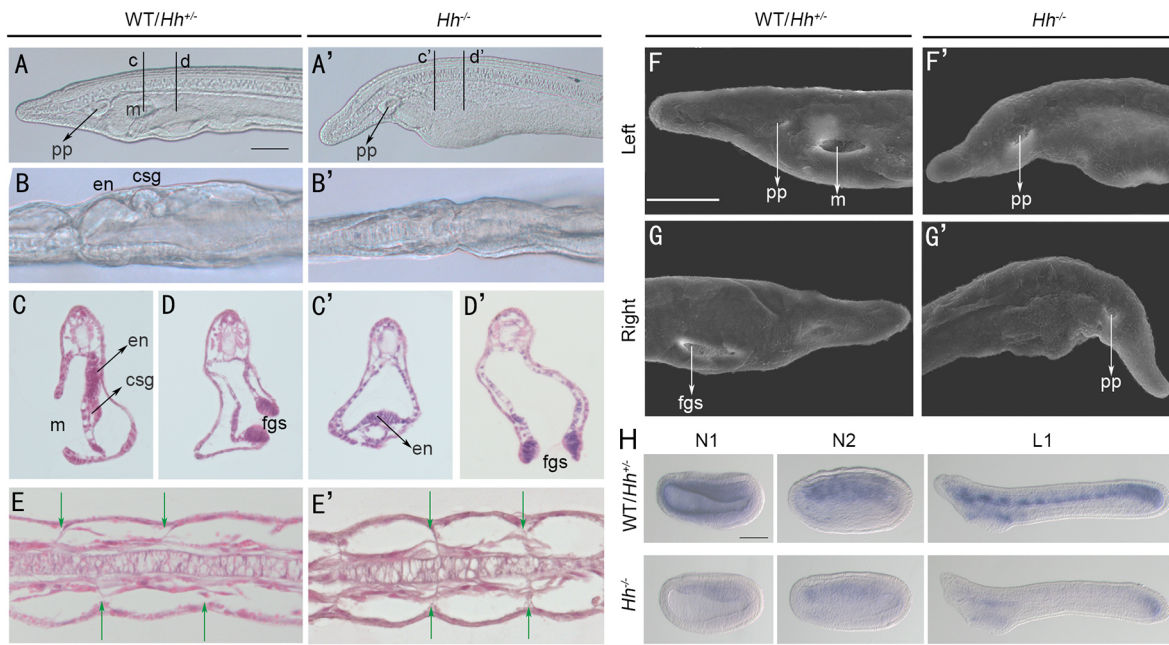
Organ-specific gene expressions in the $Hh^{-/-}$ mutant

We next examined the pattern of several asymmetrically expressed organ-specific genes in $Hh^{-/-}$ mutants and their WT/$Hh^{+/-}$ siblings. Early larvae were chosen for this analysis since major organogenesis starts at this stage and these genes display an asymmetric expression pattern in the pharyngeal region. In agreement with the above morphological observations, the expression patterns of all examined genes were changed in $Hh^{-/-}$ mutants (Fig. 3). In WT/$Hh^{+/-}$ larvae, *FoxE4* was specifically expressed in the CSG; *Krox* was strictly limited to within the CSG glandular region; *Nkx2.1* was predominantly expressed in the right side of the endostyle; and *Dkk1/2/4* in the left side of the pharynx where the mouth will form (Fig. 3A-H). However, in $Hh^{-/-}$ mutants, expression of *FoxE4* and *Krox* in the CSG glandular region was lost, and that of *FoxE4* in the CSG duct was symmetrical on both sides (Fig. 3B′,D′). Likewise, *Nkx2.1* expression faded out in the right-side endostyle of $Hh^{-/-}$ mutants, whereas that in the left side was duplicated and became symmetric (Fig. 3F′). Interestingly, the expression domain of *Dkk1/2/4* in the preordained mouth opening region appeared on both sides in the mutants (Fig. 3H′). This indicated that, like the left-side organs described above, the mouth primordium is also ectopically formed on the right side in $Hh^{-/-}$ mutants. In addition, we detected another gene, *Err*, which was asymmetrically expressed in a staggered pattern of somites and dorsal compartment motor neurons of WT larvae (Bardet et al., 2005). *Err* expression became bilaterally symmetric in the somites and dorsal compartment motor neurons of $Hh^{-/-}$ mutants (Fig. 3I,I′). These results confirmed the above morphological observations and demonstrated the requirement of *Hh* in amphioxus asymmetric organ development.

Considering the fact that Hh signaling is involved in dorsoventral patterning of the central nervous system (CNS) and somites in vertebrates (Hammerschmidt et al., 1997), we examined eight CNS/notochord/somite marker genes, namely *Wnt3*, *Pax2/5/8*, *Nkx2.1*, *m-actin*, *MRF2*, *Zic*, *Netrin* and *Brachyury*, to determine whether they are affected in the *Hh* knockout. In WT neurula, expression of *Wnt3* and *Pax2/5/8* is restricted to the dorsal part of the neural tube and that of *Nkx2.1* is confined to the ventral area of the neural tube (Kozmik et al., 1999; Schubert et al., 2001; Venkatesh et al., 1999), and these patterns appeared unaffected in $Hh^{-/-}$ embryos (Fig. 4A′-F′, Fig. S1). Similarly, the expression of *Netrin* and *Brachyury* in notochord (Holland et al., 1995; Shimeld, 2000), *m-actin* and *MRF2* in myotomes and *Zic* in the somite dorsolateral wall (Gostling and

Fig. 2. Symmetric phenotype in amphioxus larvae after *Hh* knockout. (A,A′) Left lateral view of L2 stage larva. m, mouth; pp, preoral pit. Black lines indicate the section planes in C-D′. (B,B′) Dorsal view of L2 stage larva. en, endostyle; csg, club-shaped gland. (C-D′) Sections of L2 stage larva showing asymmetrical positioning of pharyngeal organs in WT/*Hh*$^{+/-}$ embryos and symmetrical positioning in *Hh*$^{-/-}$ embryos. In WT/*Hh*$^{+/-}$ embryos, the mouth (m) opens on the left side, first gill slit (fgs) on the right side, and the dorsal part of the endostyle and CSG are formed on the right side. (E,E′) Longitudinal sections of L2 stage larva showing myotome arrangement. Arrows mark the boundary between myotomes. (F-G′) SEM images of L2 stage larva. *Hh* knockout results in the absence of a mouth opening and duplicated preoral pits. (H) Expression of *Ptch* in N1 to L1 stage larvae visualized by WISH. N1, early neurula stage; N2, mid-neurula stage; L1, early larva stage. A-B′ are bright-field, C-D′ are transverse sections stained with H&E, and E,E′ are coronal sections stained with H&E. Scale bars: 100 μm in A,A′; 50 μm in F-G′; 100 μm in H.

Shimeld, 2003; Kusakabe et al., 1997; Schubert et al., 2003) were unaffected during *Hh*$^{-/-}$ embryo development, except for the change in somite staggered pattern (Fig. 4G′-P′, Fig. S1).

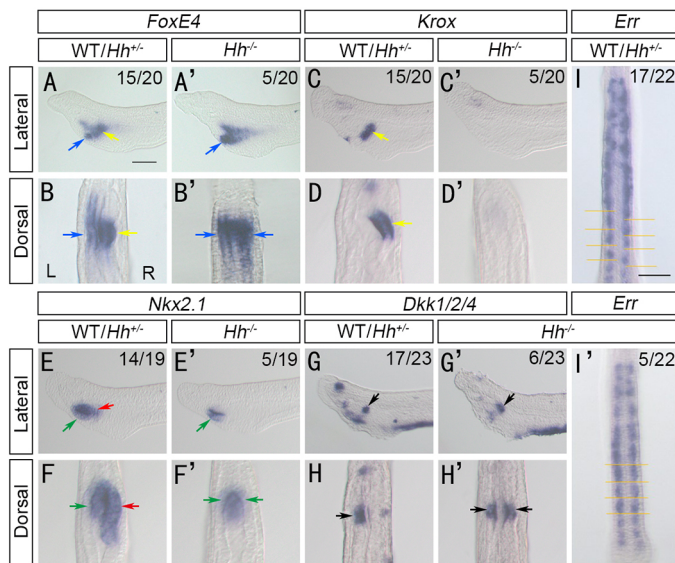### LR patterning gene expression in the *Hh* mutant

Cer, *Nodal*, *Lefty* and *Pitx2* are key players in vertebrate LR patterning. All these genes exhibit an asymmetric expression pattern during vertebrate embryonic development, with *Cer* in a right-biased manner and the other three in a left-biased fashion (Nakamura and Hamada, 2012). Orthologs of these genes in amphioxus are also asymmetrically expressed in a similar pattern to that in vertebrates (Boorman and Shimeld, 2002; Le Petillon et al., 2013; Yu et al., 2002). Recent reports further indicated that both Cer and Nodal signaling are required for LR patterning in amphioxus and that Cer acts upstream of Nodal signaling by inhibiting its activity on the right side (Soukup et al., 2015; Li et al., 2017). To dissect the molecular mechanism of Hh signaling in amphioxus LR patterning, we compared the expression patterns of these genes in *Hh*$^{-/-}$ mutants and their WT/*Hh*$^{+/-}$ siblings at the mid-gastrula (G4), late gastrula (G5), neurula with 3-4 somites (N1) and neurula with 8 somites (N2) stages. In WT/*Hh*$^{+/-}$ embryos, the four genes were symmetrically expressed at G4 and G5 (Fig. 5A,B,E,F,I,J,M,N) and asymmetrically expressed at N1 stage, with *Cer* in an L<R manner and the other three in an L>R manner (Fig. 5C,G,K,O). At N2 stage, expression of *Nodal*, *Lefty* and *Pitx* was restricted to the left side (Fig. 5H,L,P) and that of *Cer* had moved to the midline (Fig. 5D). However, *Cer* expression was completely abolished at all four stages examined in the *Hh*$^{-/-}$ mutants (Fig. 5A′-D′), and *Nodal*, *Lefty* and *Pitx* were apparently unaffected at G4 and G5 (Fig. 5E′,F′,I′,J′,M′,N′) but became bilaterally symmetric at N1 and N2 (Fig. 5G′,H′,K′,L′,O′,P′).

Hh mRNA injection rescues *Cer* expression and LR defects of *Hh*$^{-/-}$ mutants

The above experiments highlighted an essential role of *Hh* in asymmetry development in the amphioxus embryo by regulating *Cer* expression. To validate this finding further, we injected synthesized *Hh* mRNA into unfertilized eggs from *Hh*$^{+/-}$ females and then fertilized them with *Hh*$^{+/-}$ sperm to see whether the re-expression of the *Hh* gene could rescue *Hh*$^{-/-}$ phenotypes. Based on morphological observation and genotype diagnosis, we found that the *Hh*$^{-/-}$ mutants recovered their LR asymmetry and developed almost normal morphological features after *Hh* mRNA injection (Fig. 6B′,B″). We further compared *Cer* expression between the injected and uninjected embryos. About 75% (26/35) of uninjected embryos obtained from the inbreeding of *Hh*$^{+/-}$ showed a normal *Cer* expression pattern and 25% (9/35) lost *Cer* expression, which is consistent with a Mendelian segregation ratio (3:1). However, after *Hh* mRNA injection, all of the embryos (40/40) displayed a normal *Cer* expression pattern (L<R) (Fig. 6C-D″).

Hh might not provide an asymmetric cue for *Cer* expression

After demonstrating that Hh signal is necessary for *Cer* expression in amphioxus, we then asked whether the signal also provides a cue for generating asymmetric *Cer* transcription in the embryo. We first compared the expression patterns of *Cer*, *Hh* and *Ptch* (a receptor and also a target of the Hh signaling pathway) in carefully staged embryos spanning from early gastrula to around the three-somite neurula (150 min after late gastrula) stages according to our previous report (Li et al., 2017). *Cer* transcripts were first detected in the dorsoanterior endomesoderm at late gastrula stage (0 min) in an L=R manner and then shifted to the first pair of somites in an L<R fashion from 30 min after late gastrula (Fig. 7Aa-g). *Hh*

Fig. 3. Organ-specific gene expression in Hh⁻/⁻ mutants. The expression patterns of *FoxE4*, *Krox*, *Nkx2.1*, *Dkk1/2/4* and *Err* in L1 stage larvae were revealed by *in situ* hybridization. Images are left lateral or dorsal views. L and R indicate left and right side. (A-D′) Blue arrows indicate the duct of the CSG and yellow arrows indicate the glandular region of the CSG. In *Hh⁻/⁻* larvae, the duct of CSG is duplicated on the right side and the glandular region of CSG disappears on the right. (E-F′) Green arrows indicate the left part of the endostyle and red arrows indicate the right part of the endostyle. The left part is duplicated and the right part disappears in *Hh⁻/⁻* larvae. (G-H′) Black arrows indicate the mouth region. Two mouth regions appear in *Hh⁻/⁻*. (I,I′) *Err* expression marks motor neurons and somites. Horizontal lines denote somite boundaries. Numbers at top right indicate Mendelian segregation ratios from each *Hh⁺/⁻* inbreeding. Scale bars: 100 µm.

expression was turned on earlier than *Cer* expression and first detected at early gastrula stage. After late gastrula, *Hh* expression was conspicuous in the dorsolateral endomesoderm of the embryo, which covered the *Cer* expression area. However, in contrast to *Cer*, expression of *Hh* in the dorsal endomesoderm was symmetric (Fig. 7Ba-g). As a receptor and direct target gene of Hh signaling, *Ptch* transcription started shortly after *Hh* expression. In all stages examined, *Ptch* expression domains essentially followed that of *Hh* and no signs of asymmetric expression were apparent along the LR axis (Fig. 7Ca-g). These results suggested that Hh signal might not be a direct regulator for the establishment of *Cer* asymmetric expression in amphioxus embryos.

To confirm this proposal, we then examined *Cer* expression in *Hh* mRNA-injected embryos and in *Ptch⁻/⁻* mutants (our unpublished data) at N1 stage, when *Cer* is expressed on the right in WT, both of which should lead to ectopic activation of Hh signal. If Hh signal participates in the LR asymmetric expression of *Cer*, such global activation of Hh signaling would result in *Cer* expression on both sides in *Hh* mRNA-injected embryos and *Ptch⁻/⁻* mutants. Contrary to this, *Cer* expression was still confined to the right side and the embryos developed with a normal asymmetric morphology (Fig. 7D-K, Fig. S2). Furthermore, to detect whether Hh signaling activity exists on both sides at N1 stage, we examined *Cer* expression in *Hh* knockout embryos after SB505124 Nodal inhibitor treatment, which should result in a bilaterally symmetric *Cer* expression pattern in amphioxus (Soukup et al., 2015; Li et al., 2017). The results indicated that *Cer* expression became bilaterally asymmetric after SB505124 treatment in WT/*Hh⁺/⁻* embryos, but no expression was observed in either side of *Hh⁻/⁻* mutants (Fig. 8). Taken together, these results demonstrated that *Hh* regulates *Cer* expression without LR bias.

Mechanism of *Cer* regulation by Hh

We identified a canonical Gli binding sequence (5′-GACCACCCA-3′) 66 bp upstream of the *Cer* transcription initiation site in the amphioxus genome, like that in zebrafish (Wang et al., 2013). Comparative genomic analysis showed that this sequence was completely conserved among three amphioxus species: *Branchiostoma floridae*, *B. belcheri* and *Epigonichtys cultellus*. To test whether this Gli binding sequence is necessary for initiating downstream gene expression, we cloned a 1.1 kb DNA segment upstream of *Cer* including the Gli binding sequence and then inserted it into a luciferase reporter vector. The luciferase assay showed that the DNA segment including the Gli binding sequence could promote reporter gene expression in amphioxus embryos. However, the segment containing a mutated Gli binding site also promoted reporter gene expression (Fig. S3), indicating that this canonical Gli binding sequence is not required for *Cer* expression.

DISCUSSION

In the present study, we reveal that *Hh* knockout in amphioxus disrupts the placement of asymmetric organs along the LR axis and changes the expression pattern of asymmetric genes, highlighting a novel mode of *Hh* participation in early LR asymmetry development of amphioxus embryos. Combining the current data with the previous finding that Cer acts as an upstream antagonist of Nodal signaling (Li et al., 2017), we propose a model to explain how *Hh* functions in the establishment of amphioxus LR asymmetry.

Hh and the LR asymmetry development of amphioxus

That Hh signaling is involved in LR patterning was first demonstrated in chick. During chick embryo development, *Shh* expression is confined to the left side of Hensen's node at stage 4⁺. Blocking or ectopic activation of Shh function disrupts the LR patterning of heart (Levin et al., 1995). In addition, blocking Shh activity at the left side of the node inhibits *cNR-1* expression in the left LPM, and ectopic activation of Shh at the right side of the node leads to ectopic activation of *cNR-1* in the right LPM (Levin et al., 1995; Pagán-Westphal and Tabin, 1998). These findings indicated that *Shh-Nodal* signal is important for normal LR asymmetry development in chick. In mouse embryos, *Hh* and *Ptch1* are expressed bilaterally; nevertheless, *Shh⁻/⁻* or *Shh-Ihh* compound mutants or *Smo* mutants exhibit an absence of *Nodal* expression in the LPM and of heart looping (Tsukui et al., 1999; Zhang et al., 2001). Further study showed that the initiation and propagation of asymmetric *Nodal* expression in the LPM did not require Hh signal at the node, but depended on the Hh activity in the LPM (Tsiairis and McMahon, 2009). Hh signaling also functions in a similar way in the LR asymmetry development of sea urchin embryos, and *Hh* knockdown by morpholino resulted in the loss of *Nodal* expression in the right lateral ectoderm but did not affect the initial asymmetric *Nodal* expression in the right coelomic pouch (Warner et al., 2016). Together, these results indicate that *Hh* is necessary for *Nodal* expression or, in other words, that Hh signaling affects asymmetry development via controlling *Nodal* expression.

In amphioxus, preliminary studies on *Hh* expression suggested that it might not be essential for LR patterning since the onset of *Hh* asymmetric expression occurs long after that of *Nodal* (Shimeld, 1999; Yu et al., 2002). However, our observations support a crucial role of Hh signal in amphioxus LR asymmetry. We demonstrated that amphioxus larvae develop an abnormal symmetric phenotype after *Hh* is knocked out (Wang et al., 2015). All *Hh* mutants duplicated their left-side organs and lost right-side organs (Fig. 2). Moreover, loss of Hh function disrupted the expression pattern of asymmetric genes such
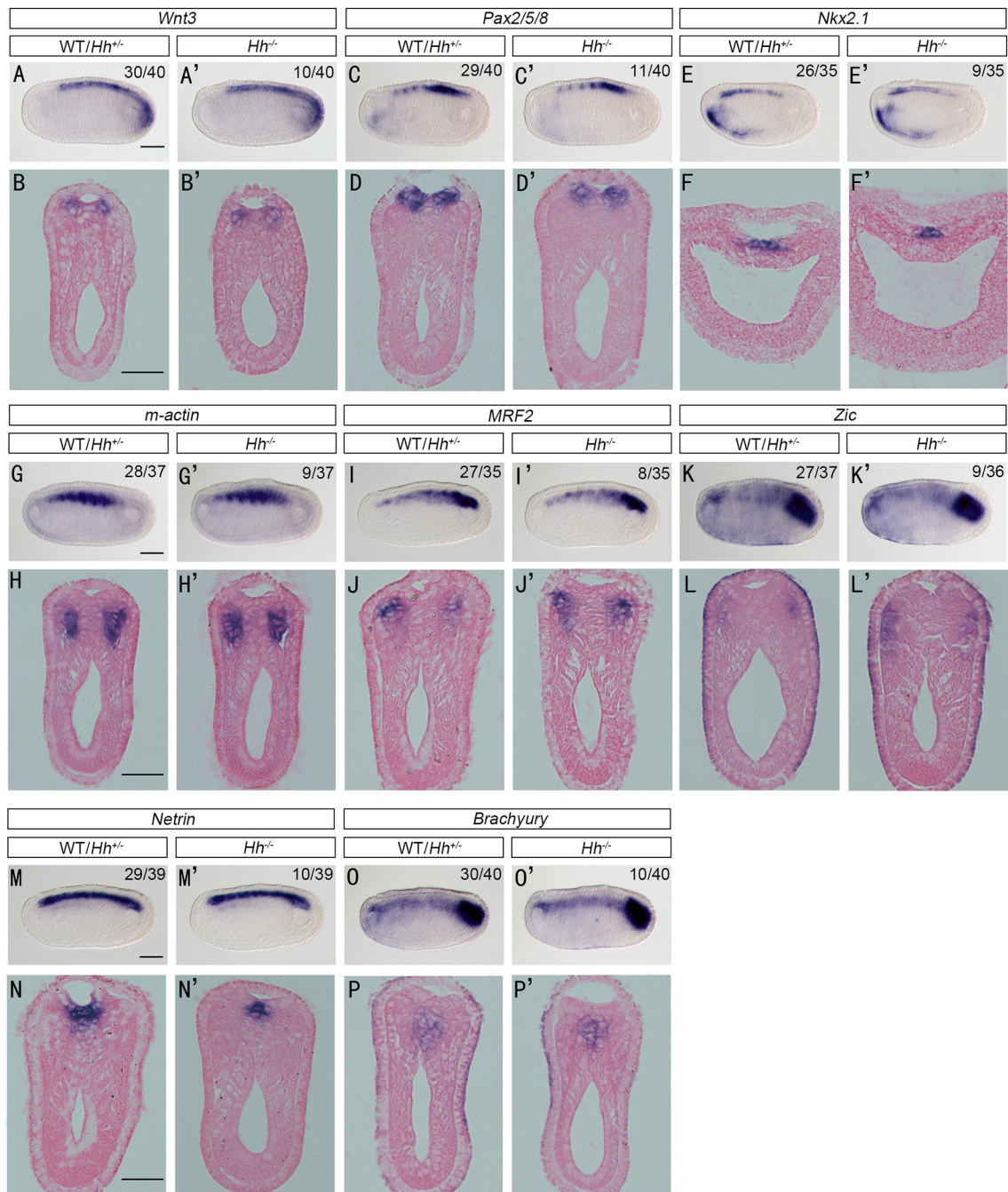
Fig. 4. Expression pattern of midline structure and somite-specific genes in Hh⁻/⁻ embryos. In WT/Hh⁺/⁻ embryos, *Wnt3* is expressed throughout the hindbrain and spinal cord, *Pax2/5/8* throughout the spinal cord, *Nkx2.1* in the ventral part of the neural tube, *m-actin* in somites, *MRF2* in the somite medial wall, *Zic* in the dorsolateral somites, *Netrin* in the neural tube and notochord, and *Brachyury* in the notochord and tailbud. None of these gene expression patterns was affected in Hh⁻/⁻ embryos. WISH (anterior left) and transverse section *in situ* hybridization at mid-neurula (8-somite) stage. Numbers at top right indicate Mendelian segregation ratios from each Hh⁺/⁻ inbreeding. Scale bars: 100 µm in A for whole mounts; 20 µm in B for sections.

as *Cer*, *Nodal*, *Lefty* and *Pitx*. We conclude that *Hh* indeed participates in LR pattern formation during amphioxus embryo development.

Cer expression in Hh knockout amphioxus

Cer is the earliest asymmetrically expressed gene in developing embryos of amphioxus and vertebrates (Marques et al., 2004; Schweickert et al., 2010). The mechanism regulating *Cer* expression remains largely unknown, although a recent study in mouse indicated that the LR asymmetry of *Cerl2* expression is determined post-transcriptionally by unilateral decay of *Cerl2* mRNA on the left

side (Nakamura et al., 2012). In our study, we showed that *Hh* knockout abolished *Cer* expression in developing amphioxus embryos from gastrula stage, suggesting that Hh signal is required for *Cer* gene expression. However, the mechanism by which Hh signaling regulates *Cer* expression remains to be elucidated, but appears not to involve a canonical Gli binding sequence that we identified in the *Cer* promoter region.

Additionally, WISH revealed that *Cer* is expressed asymmetrically in amphioxus embryos 30 min after late gastrula stage, when *Hh* and *Ptch* exhibit a symmetric expression pattern
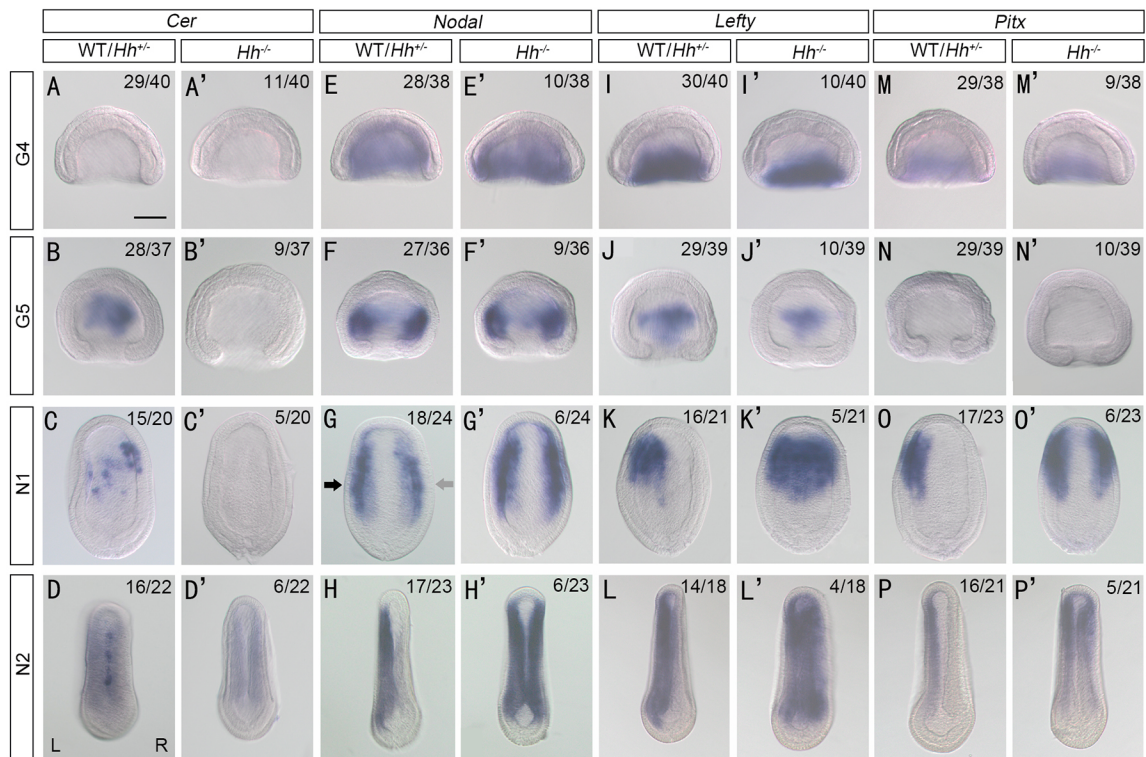
Fig. 5. Expression of LR patterning genes in amphioxus embryos. (A-P) Normal expression patterns of *Cer* (A-D), *Nodal* (E-H), *Lefty* (I-L) and *Pitx* (M-P) in WT/*Hh*^+/−^ embryos from G4 to N2 stage. (G) The black arrow indicates strong *Nodal* expression on the left and the gray arrow weak expression on the right. (A′-D′) *Cer* expression disappears in *Hh*^−/−^ embryos. (E′-H′) The normally asymmetrical expression of *Nodal* initiating from N1 stage is altered in *Hh*^−/−^ embryos. (I′-L′) The normally asymmetrical expression patterns of *Lefty* at N1 and N2 are changed into bilaterally symmetrical patterns in *Hh*^−/−^ embryos. (M′-P′) *Pitx* expression is changed into a bilaterally symmetrical pattern at N1 and N2 in *Hh*^−/−^ embryos. Dorsal views. Numbers at top right indicate Mendelian segregation ratios from each *Hh*^+/−^ inbreeding. Scale bar: 100 µm.

(Fig. 7Aa-Cg). Moreover, *Cer* expression was still confined to the right side at N1 stage when Hh signaling was constitutively activated by *Ptch* knockout or *Hh* mRNA injection. We also showed that in embryos treated with the Nodal inhibitor SB505124, bilateral *Cer* expression appeared in WT/*Hh*^+/−^ embryos but was not present in *Hh*^−/−^ embryos (Fig. 8), demonstrating that Hh signal was activated on both sides. These results suggested that Hh is necessary for *Cer* expression but that it might not provide the asymmetric cue.

Hh regulates LR asymmetric development via controlling *Cer* expression

As discussed above, *Hh* has been shown to participate in the development of asymmetry in chick, mouse or sea urchin embryos via controlling *Nodal* expression. However, our results indicate that a different situation exists in amphioxus as *Hh*^−/−^ mutants express *Nodal*, *Lefty* and *Pitx* but with a bilaterally symmetric expression pattern (Fig. 5), demonstrating that these genes do not need Hh for activation in amphioxus embryos. Similar abnormal expression of these genes was also observed in *Cer*^−/−^ amphioxus (Li et al., 2017). Moreover, *Hh* mRNA injection revealed that *Cer* expression could be recovered in *Hh*^−/−^ mutants and that the morphological asymmetry of these larvae was also rescued (Fig. 6). *Cer* encodes an antagonist of Nodal signaling and inhibits its action on the right side, which results in the expression of *Nodal* and of its targets *Lefty* and *Pitx* on the left side only (Nakamura and Hamada, 2012). Therefore, the abnormal LR patterning observed in *Hh*^−/−^ mutants can be explained by the absence of *Cer* expression.

Based on these results together with previous reports, we propose a new model for *Hh* participation in LR asymmetry development of amphioxus embryos (Fig. 9). In this model, *Hh* controls LR asymmetric morphogenesis by regulating the expression of *Cer* rather than of *Nodal*. In WT/*Hh*^+/−^ embryos, Hh signaling continually induces *Cer* expression from late gastrula stage (G5). When embryos develop into early neurula stage, *Cer* expression shifts to the right side due to some unknown factor inhibiting *Nodal* expression on the right, which results in normal LR patterning (Li et al., 2017). When *Hh* is knocked out, *Cer* expression is abolished. Hence, *Nodal* expression becomes bilaterally symmetric in the absence of inhibition by *Cer* on both sides. Thus, abnormal LR patterning occurs, with left-side organ duplication and loss of right-side structures.

The model tells us that *Hh* participates in the asymmetric development of amphioxus embryos via activation of *Cer* but that it might not provide the LR signal for *Cer* expression. In some vertebrates, such as mouse (Marques et al., 2004), frog (Schweickert et al., 2010), zebrafish and medaka (Hojo et al., 2007; Lopes et al., 2010), cilia-generated flow in the LR organizer provides the signal for asymmetric *Cer* expression. In amphioxus, cilia movement might play some roles in symmetry breaking, because ciliogenesis and embryonic rotation appear just prior to the onset of *Cer* asymmetric expression (Soukup et al., 2015). However, there is as yet no direct evidence to support that *Cer* symmetry breaking is related to cilia movement. SB505124 treatment alters the asymmetric expression pattern of *Cer* in amphioxus (Soukup et al., 2015; Li et al., 2017). Therefore, whether Nodal signaling plays roles in symmetry breaking is worthy of further study. Knockout of genes required for ciliogenesis or in the Nodal signaling pathway using gene editing (Li et al., 2014) should provide insight into this issue.
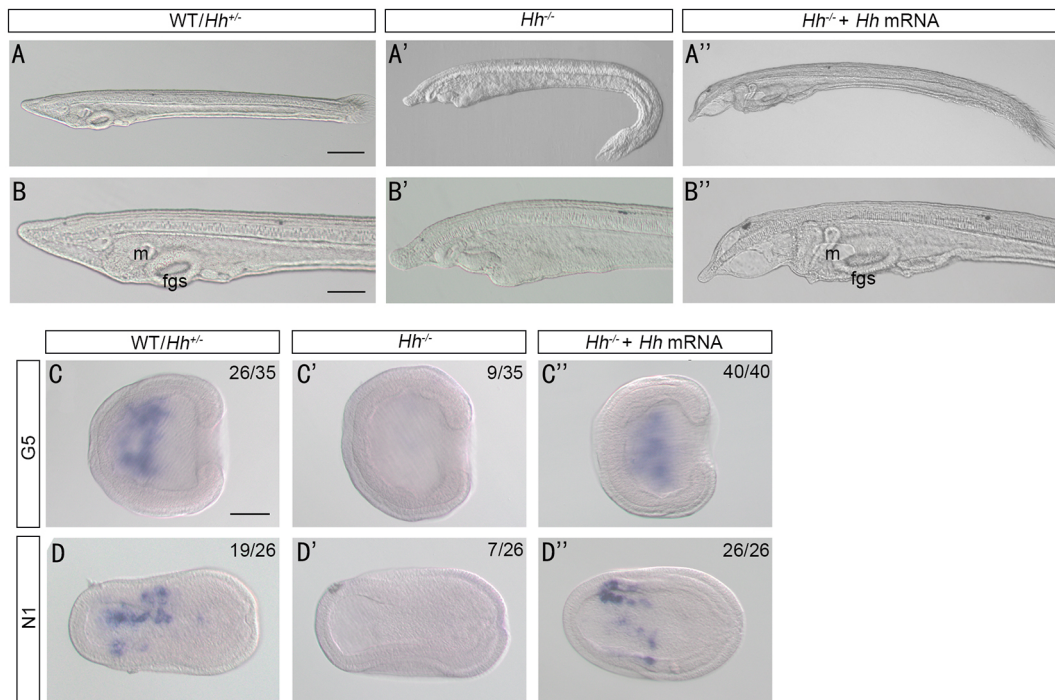
Fig. 6. Hh mRNA injection rescues the morphological defects and _Cer_ expression of _Hh_$^{-/-}$ amphioxus. (A,B) Normal phenotype of an amphioxus larva at L2 stage, with two gill slits. (A′,B′) Asymmetric arrangement of the pharyngeal organ in an _Hh_$^{-/-}$ larva. The mouth is lost and the first gill silt moves to ventral. (A″,B″) Morphological restoration in _Hh_$^{-/-}$ larvae after _Hh_ mRNA injection. m, mouth; fgs, the first gill slit on the right. A-A″ are magnified in B-B″. (C,D) _Cer_ expression in WT/_Hh_$^{+/-}$ embryos at G5 and N1 stages. (C′,D′) _Hh_ knockout results in the loss of _Cer_ expression. (C″,D″) Injection of _Hh_ mRNA induces _Cer_ expression in _Hh_ mutant embryos. WISH, dorsal views. Numbers at top right indicate Mendelian segregation ratios from each _Hh_$^{+/-}$ inbreeding. Scale bars: 100 μm in A for A-A″, C for C-D′; 50 μm in B for B-B″.

Hh signaling and mouth opening in amphioxus

In contrast to vertebrates, the amphioxus mouth opens on the left at the larval stage. This has led to controversy over whether the amphioxus mouth is a homolog of the vertebrate mouth (Kaji et al., 2016; Soukup et al., 2015). In vertebrates, Hh signaling is necessary and sufficient to initiate mouth formation, and its activity is required in a dose-dependent way to determine mouth size (Tabler et al., 2014). A recent study in amphioxus reported that the formation of the mouth was controlled by Nodal signaling (Kaji et al., 2016). However, in _Hh_$^{-/-}$ amphioxus embryos, _Nodal_, _Lefty_ and _Pitx_ were symmetrically expressed on both sides due to the loss of _Cer_ expression, and the larvae had no mouth opening on either side. However, _Cer_$^{-/-}$ amphioxus embryos also expressed _Nodal_, _Lefty_ and _Pitx_ symmetrically but two mouths appeared, one on each side (Li et al., 2017). The different mouth phenotypes of _Cer_$^{-/-}$ and _Hh_$^{-/-}$ mutants indicated that Hh signal is necessary for amphioxus mouth formation. Notably, WISH revealed that the oral mesovesicle (the definitive source of a larval mouth in amphioxus) marker genes _Dkk1/2/4_ and _Pou4_ were still expressed normally in _Hh_$^{-/-}$ larvae (Fig. 3G-H′, Fig. S4), similarly to _Cer_$^{-/-}$ mutants (Li et al., 2017). This implies that Hh is required for mouth opening, but not oral mesovesicle formation, in amphioxus. Moreover, upregulating Hh signaling activity by _Hh_ mRNA injection or _Ptch_ knockout led to an increase in the size of the larval mouth (Fig. S2). These results provide molecular evidence of an orthologous relationship of the mouth between amphioxus and vertebrates.

MATERIALS AND METHODS
Experimental animals

Amphioxus _Branchiostoma floridae_ originally introduced from Dr Jr-Kai Yu's laboratory (Institute of Cellular and Organismic Biology, Academia Sinica, Taiwan) was bred in our aquarium as described previously (Li et al.,

2012). Thermal induction spawning, egg fertilization and embryo culture were carried out according to our previous reports (Li et al., 2013, 2015; Zhang et al., 2007). Embryos and larvae at required developmental stages were fixed with 4% paraformaldehyde (PFA) in MOPS buffer (pH 7.4) at 4°C overnight. Stages were defined as mid-gastrula (G4), late gastrula (G5), pre-hatching neurula (N0), early neurula (N1), mid-neurula (N2), late neurula (N3), early larva (L1) and mouth-open larva (L2) in accordance with previous reports (Hirakow and Kajita, 1991; Hirakow and Kajita, 1994; Lu et al., 2012).

Genotyping of Hh knockout amphioxus

_Hh_ gene knockout amphioxus were generated previously using the TALEN method (Wang et al., 2015). Briefly, a pair of TALENs recognizing exon 1 of the amphioxus _Hh_ gene (Fig. 1A) were designed and assembled as described (Li et al., 2014). The resulting plasmids were linearized with _Sac_I and the TALEN mRNA synthesized using the mMESSAGE mMACHINE T3 Transcription Kit (Ambion).

TALEN mRNA was microinjected into unfertilized eggs, which were then fertilized. One day after injection, genomic DNA was isolated from the injected embryos and used as template for PCR. The PCR products were digested with _Bsr_GI to estimate the somatic mutation ratio. To obtain germline mutants, the TALEN-injected embryos (F$_0$) were raised to adulthood and crossed with WT amphioxus. The progeny (F$_1$) were genotyped using a PCR/sequencing assay. In this study, homozygous mutants (_Hh_$^{-/-}$) were obtained from the inbreeding of heterozygotes, as _Hh_$^{-/-}$ mutants cannot survive to adult. Genotyping of offspring was carried out using the PCR product cleavage assay. Primers AmphiHhF2/R2 used for this amplification respectively match the upstream/downstream sequences of the TALEN target site (Table S1). Amplicons were digested with _Bsr_GI and then subjected to agarose gel electrophoresis to distinguish genotypes: those containing the mutation were indigestible owing to loss of this restriction site, whereas those from WT were cleaved into short fragments.

Scanning electron microscopy (SEM)

Samples were prepared using the t-butyl alcohol freeze-drying method (Inoué and Osatake, 1988). First, embryos at L2 stage were fixed in 2.5%
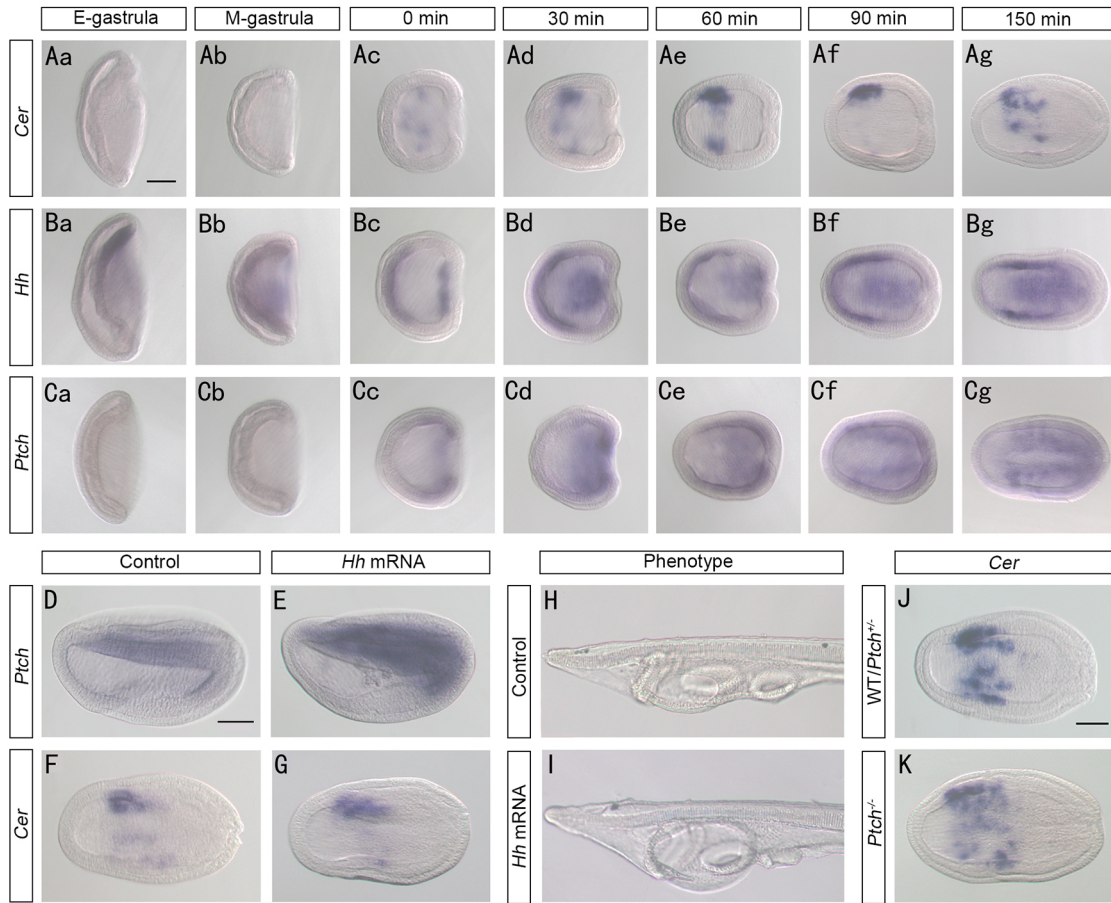
Fig. 7. The expression of *Cer*, *Hh* and *Ptch* in developing amphioxus embryos. (Aa-Cg) Dynamic *Cer* expression (Aa-g), symmetric *Hh* expression (Ba-g), and symmetric *Ptch* expression (Ca-g) patterns at seven stages of development. (D-G) The expression patterns of *Ptch* and *Cer* after *Hh* mRNA injection at N1 stage. (H,I) The phenotype of amphioxus after *Hh* mRNA injection. (J,K) *Cer* expression in *Ptch* knockout versus control embryos at N1 stage. Time is relative to late gastrula stage (defined as 0 min). Anterior is left. Scale bars: 100 µm.

glutaraldehyde in filtered PBS (pH 7.4) at 4°C overnight. Next day, the fixed samples were washed three times in 1 M PBS for 10 min each, and then dehydrated in a graded ethanol series. Specimens were then transferred into 100% t-butyl alcohol, and the liquid was changed five times at 10 min intervals. Finally, specimens were immersed in t-butyl alcohol at 4°C overnight. Next day, the specimens were dried in a vacuum freeze dryer, mounted on an aluminium stub, coated with platinum and observed under a JSM-6390 field emission scanning electron microscope (JEOL) at 20 kV.

### Whole-mount *in situ* hybridization (WISH) and histology

RNA probes were amplified using the primers listed in Table S1. cDNA templates for PCR were derived from total RNA extracted from mixed embryos and larvae. PCR products were cloned into the pGEM-T Easy vector (Promega) and transformed into *E. coli*. After sequencing verification, digoxigenin (DIG)-labeled antisense probes were synthesized for target genes using SP6 or T7 RNA polymerase (depending on insert orientation). WISH was performed according to Holland et al. (1996) with slight modifications as follows: the duration of proteinase K treatment varied from 3 to 10 min depending on embryonic stage, and probe incubation was performed at 65°C overnight.

After imaging as whole mounts, embryos were embedded in 1% agarose (in 0.5 M PBS), then dehydrated in an ethanol series (30%, 50%, 60%, 70%, 80%, 95% and 100%, 10 min each). Finally, the embryos were embedded in paraffin, sectioned at 5 µm, mounted on a polylysine-treated slide and stained with Eosin according to standard histological methods.

Hh mRNA synthesis and microinjection

Full-length amphioxus *Hh* cDNA was amplified using primers AmphiHhF1/R1 (Table S1) and the purified cDNA fragment subcloned
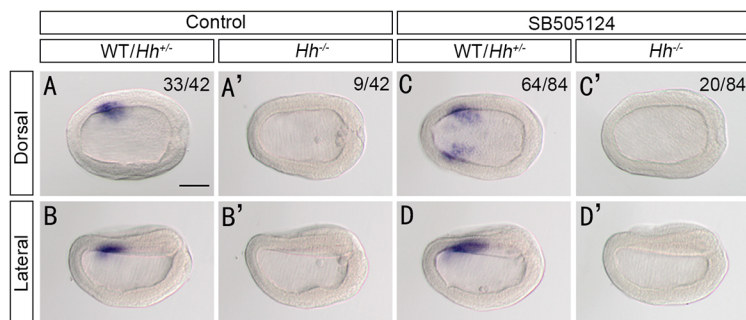
Fig. 8. *Cer* expression requires Hh signaling. (A,B) *Cer* expression in WT/*Hh*^{+/−} embryos. (A′,B′) *Hh* knockout abolishes *Cer* expression. (C,D) Treatment with the Nodal inhibitor SB505124 results in bilateral expression of *Cer* in WT/*Hh*^{+/−} embryos. (C′,D′) *Cer* expression remains absent in *Hh*^{−/−} embryos after SB505124 treatment. Numbers at top right indicate Mendelian segregation ratios from each *Hh*^{+/−} inbreeding. Scale bar: 100 µm.
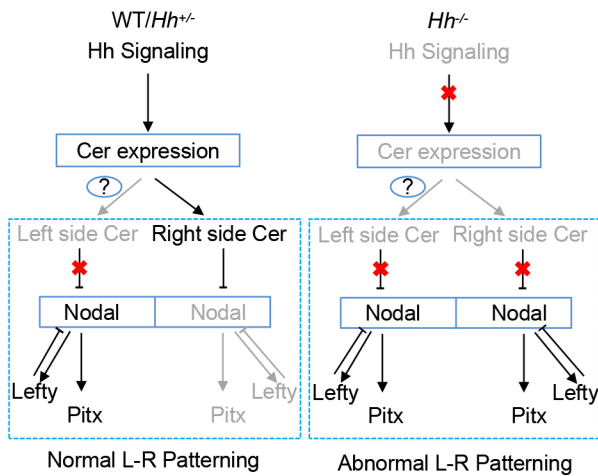
Fig. 9. Model of *Hh* function in amphioxus LR pattering. In WT or *Hh*^{+/−} amphioxus, Hh signal initially induces *Cer* expression in both sides of early embryos. Then, *Cer* expression in the left side is inhibited by unknown factors, removing the inhibition of *Nodal* gene expression on this side. These unknown factors are not present in the right side of embryos, where *Cer* expression continues to inhibit *Nodal* expression. Thus, embryos develop a normal asymmetric pattern. In *Hh* knockout amphioxus, no *Cer* expression takes place due to the lack of Hh signaling and *Nodal* expression continues in both sides, leading to the abnormal LR patterning of embryos. Gray text denotes inhibition of factor expression.

into the Addgene plasmid pXT7. After sequencing verification, we synthesized capped *Hh* mRNA using the mMESSAGE mMACHINE T7 Transcription Kit (Ambion) and stored the mRNA at −80°C until use.

Unfertilized eggs and sperm were obtained separately using the heat-shock method (Li et al., 2013) and *Hh* mRNA mixed with red fluorescent dye was injected into unfertilized eggs as described (Liu et al., 2013). The final concentration of *Hh* mRNA was 1.5 μg/μl, and the injection dose was 2 pl for each egg. After injection, the eggs were fertilized with preserved sperm, and any unfertilized eggs or those without red fluorescence sorted out under a fluorescence microscope. The remaining eggs were cultured in an incubator at 25°C and 95% humidity. Samples were collected for *in situ* hybridization at the desired developmental stages.

References
Bardet, P.-L., Schubert, M., Horard, B., Holland, L. Z., Laudet, V., Holland, N. D. and Jean-Marc, V. (2005). Expression of estrogen-receptor related receptors in amphioxus and zebrafish: implications for the evolution of posterior brain segmentation at the invertebrate-to-vertebrate transition. *Evol. Dev.* **7**, 223-233.

Bertrand, S. and Escriva, H. (2011). Evolutionary crossroads in developmental biology: amphioxus. *Development* **138**, 4819-4830.

Boorman, C. J. and Shimeld, S. M. (2002). Pitx homeobox genes in *Ciona* and amphioxus show left-right asymmetry is a conserved chordate character and define the ascidian adenohypophysis. *Evol. Dev.* **4**, 354-365.

Brennan, J., Norris, D. P. and Robertson, E. J. (2002). Nodal activity in the node governs left-right asymmetry. *Genes Dev.* **16**, 2339-2344.

Chen, J. N., Van Eeden, F. J., Warren, K. S., Chin, A., Nusslein-Volhard, C., Haffter, P. and Fishman, M. C. (1997). Left-right pattern of cardiac *BMP4* may drive asymmetry of the heart in zebrafish. *Development* **124**, 4373-4382.

Dathe, V., Gamel, A., Männer, J., Brand-Saberi, B. and Christ, B. (2002). Morphological left-right asymmetry of Hensen's node precedes the asymmetric expression of *Shh* and *Fgf8* in the chick embryo. *Anat. Embryol.* **205**, 343-354.

Gostling, N. J. and Shimeld, S. M. (2003). Protochordate *Zic* genes define primitive somite compartments and highlight molecular changes underlying neural crest evolution. *Evol. Dev.* **5**, 136-144.

Hammerschmidt, M., Brook, A. and McMahon, A. P. (1997). The world according to hedgehog. *Trends Genet.* **13**, 14-21.

Hirakow, R. and Kajita, N. (1991). Electron microscopic study of the development of amphioxus, *Branchiostoma belcheri tsingtauense*: the gastrula. *J. Morphol.* **207**, 37-52.

Hirakow, R. and Kajita, N. (1994). Electron microscopic study of the development of amphioxus, *Branchiostoma belcheri tsingtauense*: the neurula and larva. *Acta Anat. Nippon* **69**, 1-13.

Hojo, M., Takashima, S., Kobayashi, D., Sumeragi, A., Shimada, A., Tsukahara, T., Yokoi, H., Narita, T., Jindo, T. and Kage, T. (2007). Right-elevated expression of *charon* is regulated by fluid flow in medaka Kupffer's vesicle. *Dev. Growth Differ.* **49**, 395-405.

Holland, P. W., Koschorz, B., Holland, L. Z. and Herrmann, B. G. (1995). Conservation of *Brachyury* (T) genes in amphioxus and vertebrates: developmental and evolutionary implications. *Development* **121**, 4283-4291.

Holland, L. Z., Holland, P. W., Holland, N. D., Ferraris, J. D. and Palumbi, S. R. (1996). Revealing homologies between body parts of distantly related animals by in situ hybridization to developmental genes: amphioxus vs vertebrates. In *Molecular Zoology: Advances, Strategies, and Protocols* (ed. J. D. Ferraris and S. R. Palumbi), pp 267-282, 473-483. New York: Wiley-Liss.

Hooper, J. E. and Scott, M. P. (2005). Communicating with Hedgehogs. *Nat. Rev. Mol. Cell Biol.* **6**, 306-317.

Inoué, T. and Osatake, H. (1988). A new drying method of biological specimens for scanning electron microscopy: the t-butyl alcohol freeze-drying method. *Arch. Histol. Cytol.* **51**, 53-59.

Kaji, T., Reimer, J. D., Morov, A. R., Kuratani, S. and Yasui, K. (2016). Amphioxus mouth after dorso-ventral inversion. *Zool. Lett.* **2**, 2.

Koop, D. and Holland, L. Z. (2008). The basal chordate amphioxus as a simple model for elucidating developmental mechanisms in vertebrates. *Birth Defects Res. C Embryo Today* **84**, 175-187.

Kozmik, Z., Holland, N. D., Kalousova, A., Paces, J., Schubert, M. and Holland, L. Z. (1999). Characterization of an amphioxus paired box gene, *AmphiPax2/5/8*: developmental expression patterns in optic support cells, nephridium, thyroid-like structures and pharyngeal gill slits, but not in the midbrain-hindbrain boundary region. *Development* **126**, 1295-1304.

Kusakabe, R., Kusakabe, T., Satoh, N., Holland, N. D. and Holland, L. Z. (1997). Differential gene expression and intracellular mRNA localization of amphioxus *actin* isoforms throughout development: implications for conserved mechanisms of chordate development. *Dev. Genes Evol.* **207**, 203-215.

Le Petillon, Y., Oulion, S., Escande, M.-L., Escriva, H. and Bertrand, S. (2013). Identification and expression analysis of BMP signaling inhibitors genes of the DAN family in amphioxus. *Gene Expr. Patterns* **13**, 377-383.

Levin, M., Johnson, R. L., Sterna, C. D., Kuehn, M. and Tabin, C. (1995). A molecular pathway determining left-right asymmetry in chick embryogenesis. *Cell* **82**, 803-814.

Li, G., Yang, X., Shu, Z., Chen, X. Y. and Wang, Y. Q. (2012). Consecutive spawnings of Chinese amphioxus, *Branchiostoma belcheri*, in captivity. *PLoS ONE* **7**, e50838.

Li, G., Shu, Z. H. and Wang, Y. Q. (2013). Year-round reproduction and induced spawning of Chinese amphioxus, *Branchiostoma belcheri*, in laboratory. *PLoS ONE* **8**, e75461.

Li, G., Feng, J., Lei, Y., Wang, J., Wang, H., Shang, L.-K., Liu, D. T., Zhao, H., Zhu, Y. and Wang, Y. Q. (2014). Mutagenesis at specific genomic loci of amphioxus *Branchiostoma belcheri* using TALEN method. *J. Genet. Genomics* **41**, 215-219.

Li, G., Wang, J., Yuan, L., Wang, H. and Wang, Y. Q. (2015). A simple method for selecting spawning-ready individuals out from laboratorial cultured amphioxus population. *J. Exp. Zool. B Mol. Dev. Evol.* **324**, 629-635.

Li, G., Liu, X., Xing, C., Zhang, H., Shimeld, S. M. and Wang, Y. Q. (2017). Cerberus-Nodal-Lefty-Pitx signaling cascade controls left-right asymmetry in amphioxus. *Proc. Natl. Acad. Sci. USA* **114**, 3684-3689.

Liu, X., Li, G., Feng, J., Yang, X. and Wang, Y. Q. (2013). An efficient microinjection method for unfertilized eggs of Asian amphioxus *Branchiostoma belcheri*. *Dev. Genes Evol.* **223**, 269-278.

DEVELOPMENT

Lopes, S. S., Lourenço, R., Pacheco, L., Moreno, N., Kreiling, J. and Saúde, L. (2010). Notch signalling regulates left-right asymmetry through ciliary length control. *Development* **137**, 3625-3632.

Lu, T. M., Luo, Y. J. and Yu, J. K. (2012). BMP and Delta/Notch signaling control the development of amphioxus epidermal sensory neurons: insights into the evolution of the peripheral sensory system. *Development* **139**, 2020-2030.

Marques, S., Borges, A. C., Silva, A. C., Freitas, S., Cordenonsi, M. and Belo, J. A. (2004). The activity of the Nodal antagonist Cerl-2 in the mouse node is required for correct L/R body axis. *Genes Dev.* **18**, 2342-2347.

Minguillon, C. and Garcia-Fernandez, J. (2002). The single amphioxus *Mox* gene: insights into the functional evolution of *Mox* genes, somites, and the asymmetry of amphioxus somitogenesis. *Dev. Biol.* **246**, 455-465.

Nakamura, T. and Hamada, H. (2012). Left-right patterning: conserved and divergent mechanisms. *Development* **139**, 3257-3262.

Nakamura, T., Saito, D., Kawasumi, A., Shinohara, K., Asai, Y., Takaoka, K., Dong, F., Takamatsu, A., Belo, J. A. and Mochizuki, A. (2012). Fluid flow and interlinked feedback loops establish left-right asymmetric decay of *Cerl2* mRNA. *Nat. Commun.* **3**, 187-190.

Pagán-Westphal, S. M. and Tabin, C. J. (1998). The transfer of left-right positional information during chick embryogenesis. *Cell* **93**, 25-35.

Saijoh, Y., Oki, S., Ohishi, S. and Hamada, H. (2003). Left-right patterning of the mouse lateral plate requires nodal produced in the node. *Dev. Biol.* **256**, 161-173.

Sampath, K., Cheng, A. M., Frisch, A. and Wright, C. V. (1997). Functional differences among *Xenopus nodal-related* genes in left-right axis determination. *Development* **124**, 3293-3302.

Schilling, T. F., Concordet, J.-P. and Ingham, P. W. (1999). Regulation of left-right asymmetries in the zebrafish by *Shh* and *BMP4*. *Dev. Biol.* **210**, 277-287.

Schubert, M., Holland, L. Z., Stokes, M. D. and Holland, N. D. (2001). Three amphioxus *Wnt* genes (*AmphiWnt3*, *AmphiWnt5*, and *AmphiWnt6*) associated with the tail bud: the evolution of somitogenesis in chordates. *Dev. Biol.* **240**, 262-273.

Schubert, M., Meulemans, D., Bronner-Fraser, M., Holland, L. Z. and Holland, N. D. (2003). Differential mesodermal expression of two amphioxus *MyoD* family members (*AmphiMRF1* and *AmphiMRF2*). *Gene Expr. Patterns* **3**, 199-202.

Schweickert, A., Vick, P., Getwan, M., Weber, T., Schneider, I., Eberhardt, M., Beyer, T., Pachur, A. and Blum, M. (2010). The nodal inhibitor Coco is a critical target of leftward flow in *Xenopus*. *Curr. Biol.* **20**, 738-743.

Shimeld, S. M. (1999). The evolution of the hedgehog gene family in chordates: insights from amphioxus *hedgehog*. *Dev. Genes Evol.* **209**, 40-47.

Shimeld, S. M. (2000). An amphioxus netrin gene is expressed in midline structures during embryonic and larval development. *Dev. Genes Evol.* **210**, 337-344.

Soukup, V., Yong, L. W., Lu, T.-M., Huang, S.-W., Kozmik, Z. and Yu, J.-K. (2015). The Nodal signaling pathway controls left-right asymmetric development in amphioxus. *EvoDevo* **6**, 5.

Sutherland, M. J. and Ware, S. M. (2009). Disorders of left-right asymmetry: heterotaxy and situs inversus. *Am. J. Med. Genet. C Semin. Med. Genet.* **151C**, 307-317.

Tabler, J. M., Bolger, T. G., Wallingford, J. and Liu, K. J. (2014). Hedgehog activity controls opening of the primary mouth. *Dev. Biol.* **396**, 1-7.

Tsiairis, C. D. and McMahon, A. P. (2009). An Hh-dependent pathway in lateral plate mesoderm enables the generation of left/right asymmetry. *Curr. Biol.* **19**, 1912-1917.

Tsukui, T., Capdevila, J., Tamura, K., Ruiz-Lozano, P., Rodriguez-Esteban, C., Yonei-Tamura, S., Magallón, J., Chandraratna, R. A. S., Chien, K. and Blumberg, B. (1999). Multiple left-right asymmetry defects in *Shh*$^{-/-}$ mutant mice unveil a convergence of the *Shh* and retinoic acid pathways in the control of *Lefty-1*. *Proc. Natl. Acad. Sci. USA* **96**, 11376-11381.

Venkatesh, T. V., Holland, N. D., Holland, L. Z., Su, M.-T. and Bodmer, R. (1999). Sequence and developmental expression of amphioxus *AmphiNk2–1*: insights into the evolutionary origin of the vertebrate thyroid gland and forebrain. *Dev. Genes Evol.* **209**, 254-259.

Wang, X., Zhao, Z., Muller, J., Iyu, A., Khng, A. J., Guccione, E., Ruan, Y. and Ingham, P. W. (2013). Targeted inactivation and identification of targets of the *Gli2a* transcription factor in the zebrafish. *Biol. Open* **2**, 1203-1213.

Wang, H., Li, G. and Wang, Y. Q. (2015). Generating amphioxus *Hedgehog* knockout mutants and phenotype analysis. *Hereditas (Beijing)* **37**, 1036-1043.

Warner, J. F., Miranda, E. L. and McClay, D. R. (2016). Contribution of hedgehog signaling to the establishment of left-right asymmetry in the sea urchin. *Dev. Biol.* **411**, 314-324.

Yoshiba, S. and Hamada, H. (2014). Roles of cilia, fluid flow, and Ca^{2+} signaling in breaking of left-right symmetry. *Trends Genet.* **30**, 10-17.

Yu, K., Jr, Holland, L. Z. and Holland, N. D. (2002). An amphioxus nodal gene (*AmphiNodal*) with early symmetrical expression in the organizer and mesoderm and later asymmetrical expression associated with left–right axis formation. *Evol. Dev.* **4**, 418-425.

Zhang, X. M., Ramalho-Santos, M. and McMahon, A. P. (2001). Smoothened mutants reveal redundant roles for Shh and Ihh signaling including regulation of L/R asymmetry by the mouse node. *Cell* **105**, 781-792.

Zhang, Q. J., Sun, Y., Zhong, J., Li, G., Lü, X. M. and Wang, Y. Q. (2007). Continuous culture of two lancelets and production of the second filial generations in the laboratory. *J. Exp. Zool. B Mol. Dev. Evol.* **308**, 464-472.

DEVELOPMENT